Amino Acids (2015) 47:757–765
DOI 10.1007/s00726-014-1906-9

ORIGINAL ARTICLE

Green biochemistry approach for synthesis of silver and gold nanoparticles using *Ficus racemosa* latex and their pH-dependent binding study with different amino acids using UV/Vis absorption spectroscopy

Sandesh R. Tetgure · Amulrao U. Borse · Babasaheb R. Sankapal · Vaman J. Garole · Dipak J. Garole

Received: 16 September 2014 / Accepted: 16 December 2014 / Published online: 25 January 2015

Abstract Simple and eco-friendly biosynthesis approach was developed to synthesize silver nanoparticles (SNPs) and gold nanoparticles (GNPs) using *Ficus racemosa* latex as reducing agent. The presence of sunlight is utilized with latex and achieved the nanoparticles whose average size was in the range of 50–120 nm for SNPs and 20–50 nm for GNPs. The synthesized nanoparticles were characterized by UV/Visible absorption spectroscopy, X-ray diffraction, and field emission—scanning electron microscopy techniques toget understand the obtained nanoparticles. The pH-dependent binding studies of SNPs and GNPs with four amino acids, namely L-lysine, L-arginine, L-glutamine and glycin have been reported.

Handling Editor: H. S. Sharma.

Electronic supplementary material The online version of this article (doi:10.1007/s00726-014-1906-9) contains supplementary material, which is available to authorized users.

S. R. Tetgure · A. U. Borse (✉) · D. J. Garole (✉)
School of Chemical Sciences, North Maharashtra University, Jalgaon 425001, Maharashtra, India
e-mail: amulborse@gmail.com

D. J. Garole
e-mail: drdipakgarole@gmail.com

B. R. Sankapal
Nano Material and Device Laboratory, Department of Applied Physics, Visvesvaraya National Institute of Technology, Nagpur 440010, Maharashtra, India

V. J. Garole
Konkan Education Society's S.P. Jain Junior College, Nagothane 402106, Maharashtra, India

D. J. Garole
Directorate of Geology and Mining, Government of Maharashtra, Nagpur 440010, Maharashtra, India

Keywords Silver and gold nanoparticles · *Ficus racemosa* latex · Amino acids · Association constant

Introduction

There is an increasing commercial demand for the nanoparticles due to their wide applicability in various areas such as electronics, catalysis, chemistry, energy, and medicine (Basavegowda et al. 2013). Metallic nanoparticles are traditionally synthesized by wet chemical techniques, where the chemicals used are quite often toxic and flammable (Justin Packia Jacob et al. 2012). Currently, development of the environmentally benign nanoparticles synthesis processes is gaining importance as these processes does not use the toxic chemicals in the synthesis protocol (Thakkar et al. 2010). Moreover, green synthesis of different metallic nanoparticles using plant materials has successfully made an important contribution to green nanotechnology as it implements novel green chemistry approach with added advantages over chemical and physical methods: as it is environment-friendly, does not need high pressure or high temperature, and no toxic chemicals are needed in biological methods (Das and Brar 2013; Mittal et al. 2014). Medical industry uses silver and SNPs for different purposes such as topical ointments and creams to prevent infection of burns and open wounds, medical devices and implants prepared with silver-impregnated polymers (Song and Kim 2009). In addition, SNPs have found applications in various fields including electronic devices, chemical/biological sensing, and surface-enhanced Raman spectroscopy, drug delivery, and gene delivery, catalyst, antimicrobial agents, conductive coating, and sensors (Christensen et al. 2011; Dong et al. 2014; Bryaskova et al. 2010). GNPs also have become prominent for their promising

biomedical applications such as X-ray contrast agent, Cancer Nanotechnology, catalysis, biolabeling, nonlinear optical devices, and optical recording media (Cai et al. 2008; Alric et al. 2008; De et al. 2012).

Recently, several researchers reported the different biosynthesis route for precious element nanoparticles. The formation of SNPs and GNPs by living plants opened new and exciting ways to fabricate nanoparticles (Gardea-Torresdey et al. 2002, 2003). Recently, physiologically stable, bio-compatible SNPs have been synthesized by mixing the silver solution with leaf extract of *Azadirachta indica* without using any surfactant or external energy (Nazeruddin et al. 2014). Synthesis of small-sized SNPs with narrow distribution from 3 to 17 nm has been also reported (Dong et al. 2014). Moreover, SNPs were synthesized using hot water *olive* leaf extracts as reducing and stabilizing agent and evaluated for antibacterial activity against drug-resistant bacterial isolates (Khalil et al. 2013). Aqueous extract of *Lakshmi tulasi* (*Ocimum sanctum*) leaf as a reducing and stabilizing agent for synthesis of SNPs has been reported (Rao et al. 2013). The synthesis and characterization of SNPs using *Iresine herbstii* and evaluation of their antibacterial, antioxidant, and cytotoxic activity has been reported (Dipankar and Murugan 2012). The biological method for the synthesis of SNPs using *Annona squamosa* leaf extract and its cytotoxicity against MCF-7 cells has been reported (Vivek et al. 2012). SNPs with average size of 26 nm have been also synthesized by exposing aqueous silver ions to *Coriandrum sativum* leaf extract as reducing agent (Sathyavathi et al. 2010). Many plants such as *Tridax procumbens*, *Jatropha curcas*, *Solanum melongena*, *Datura metel*, and *Citrus aurantium* have been also reported for synthesis of SNPs and GNPs (Reddy et al. 2010). Leaf extracts of two plants, *Magnolia kobus* and *Diopyros kaki*, have been used for extracellular synthesis of GNPs (Song et al. 2009). GNPs in the size range of 6.75 to 57.91 nm have been prepared by exposing aqueous gold to *coriander* leaf extract (Narayanan and Sakthivel 2008). SNPs ranging from 55 to 80 nm in size and GNPs with triangular or spherical shape were fabricated by reacting the novel sundried biomass of *Cinnamomum camphora* leaf with aqueous silver or gold precursors at ambient temperature (Huang et al. 2007). SNPs have been synthesized using *Capsicum annuum* L. extract and recognition-reduction-limited nucleation and growth model was suggested to explain the possible formation mechanism (Li et al. 2007). Biomimetic synthesis of SNPs using crude *black pepper* (*Piper nigrum*) extract at room temperature has been also reported (Shukla et al. 2010). *Oat* (*Avena sativa*) biomass was studied as an alternative to recover Au(III) ions from aqueous solutions and for its capacity to reduce Au(III) to Au(0) forming GNPs (Armendariz et al. 2004). Synthesis of gold nanotriangle and SNPs using purified *phyllanthin*

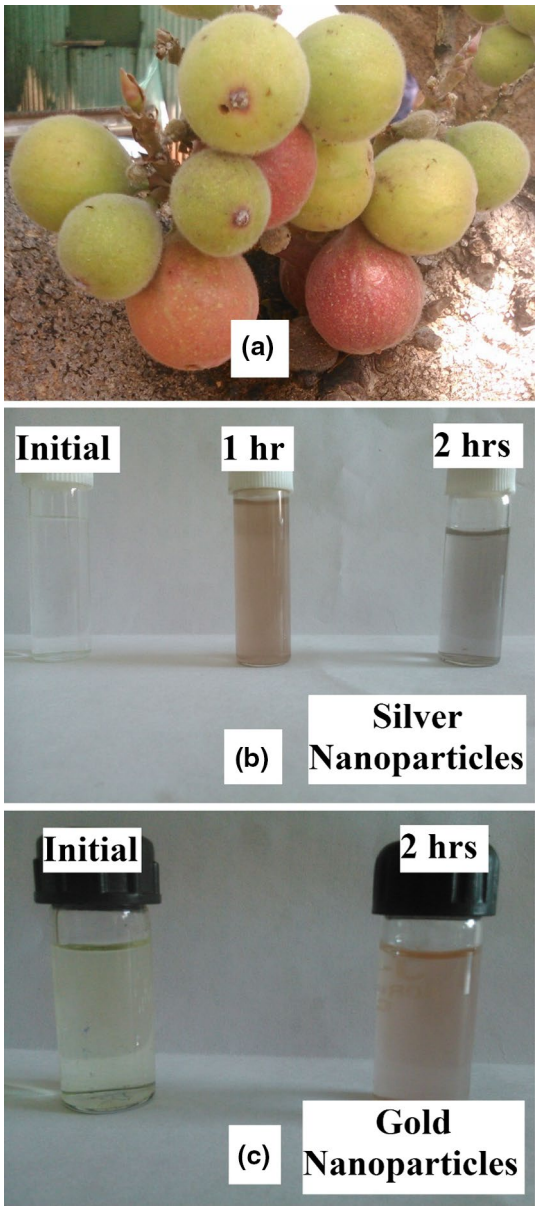

Fig. 1 **a** Plant image and color changes for **b** SNPs and **c** GNPs

extract at ambient conditions has been reported (Kasthuri et al. 2009). SNPs and GNPs have been synthesized by reducing the aqueous solution of $AgNO_3$ and $AuCl_4$ with *clove* extract (Singh et al. 2010). The fungus *Penicillium* was also used for rapid extra-/intracellular biosynthesis of GNPs (Du et al. 2011). The extracellular production of SNPs and GNPs has been carried out from the leaves of the plants, *Tridax procumbens* L. (*Coat buttons*), *Jatropa curcas* L. (*Barbados nut*), *Calotropis gigantea* L. (*Calotropis*), *Solanum melongena* L. (*Eggplant*), *Datura metel* L. (*Datura*), *Carica papaya* L. (*Papaya*), and *Citrus aurantium* L. (*Bitter orange*) by the sunlight exposure method (Rajasekharreddy et al. 2010).

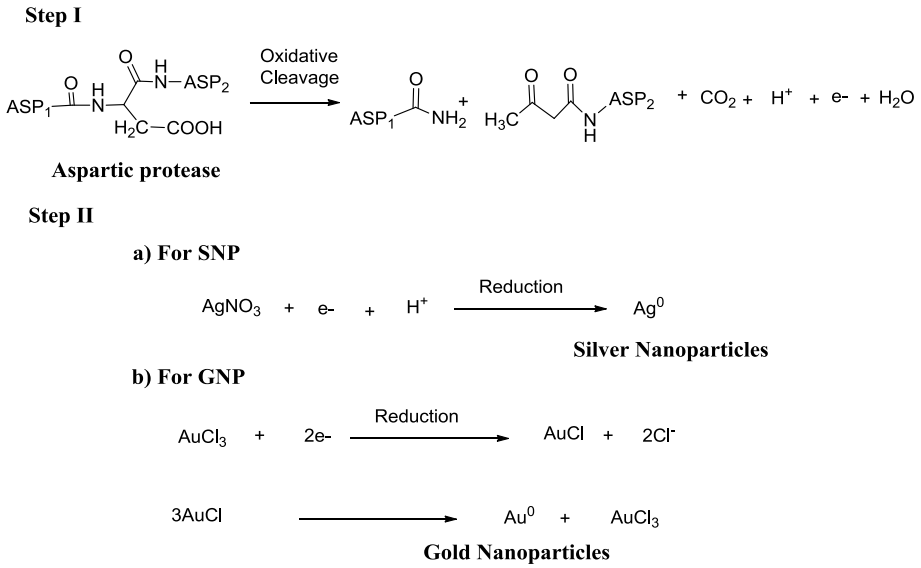

Fig. 2 Possible mechanistic pathway for synthesis of SNPs and GNPs

Biologically active molecules such as amino acids, peptides, and proteins can be attached to nanoparticles to improve their bio-specificity and different applications in the field of biological and medical sciences (Mihailescu et al. 2007). It is increasingly being recognized that amine groups can bind to nanoparticles quite strongly (Zare et al. 2010).

In this study, a simple, environmentally friendly biosynthetic approach was investigated for the preparation of SNPs and GNPs with *Ficus racemosa* latex. Nanoparticles were synthesized by mixing an aqueous solution of silver nitrate and chloroauric acid with an aqueous solution of *Ficus racemosa* latex. This complies with the green-chemistry principles of using safe synthesis. The obtained nanoparticles were comprehensively characterized via X-ray diffraction (XRD), UV/Vis spectroscopy, field emission—scanning electron microscopy (FE-SEM), and energy-dispersive X-ray spectroscopy (EDS). Prepared nanoparticles were studied for evaluation of their binding constants with different amino acids at different pH conditions using UV/Vis spectroscopy.

Materials

Reagents

- Choroauric acid (Gold(III) Chloride; http://www.lobachemie.com; Cat No. 02734 00001)

! CAUTION Choroauric acid is Corrosive. When handling these chemicals, wear suitable protective clothing, gloves and eye/face protection.

- Silver nitrate (http://www.merck.co.in; Cat No. 61763600251730)

! CAUTION Silver nitrate is Corrosive. When handling these chemicals, wear protective gloves/protective clothing/eye protection/face protection).

- L-Lysine monohydrochloride (http://www.avrasynthesis.com; Cat. No. ASL1378)
- L-Arginine (http://www.avrasynthesis.com; Cat. No. ASL1382)
- L-Glutamine (http://www.avrasynthesis.com; Cat. No. ASL1494)
- Glycin (http://www.srlchem.com; Cat. No. 0747124)

Equipment

- X-ray diffraction (XRD) patterns were recorded in the scanning angles of 20° to 80° with a Rigaku Rotalflex RU-200B diffractometer using a Cu Kα ($\lambda = 1.5418$ Å) (http://www.rigaku.com).
- Surface morphological studies were performed using field emission-scanning electron microscopy (FE-SEM) unit (S-4800 instrument from Hitachi, Japan) operated at 10 kV and elemental analysis was performed by EDS unit coupled with SEM unit (http://www.hitachi.com).
- The optical absorption spectra were recorded (i.e., in between 300 and 800 nm wavelength range) by UV/Vis spectrophotometer (Shimadzu 2450) with 1.0 cm quartz cell used for spectrophotometric measurements (http://www.shimadzu.com).
- Prepared nanoparticles were separated from liquid phase by centrifuge process using Laboratory Centrifuge Machine (REMI R4C) at 3,000 rpm for 1 h (http://www.remilabworld.com).

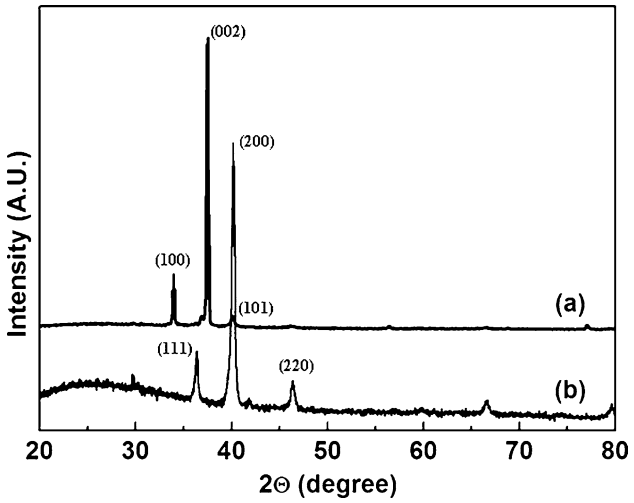

Fig. 3 XRD pattern for *a* SNPs and *b* GNPs

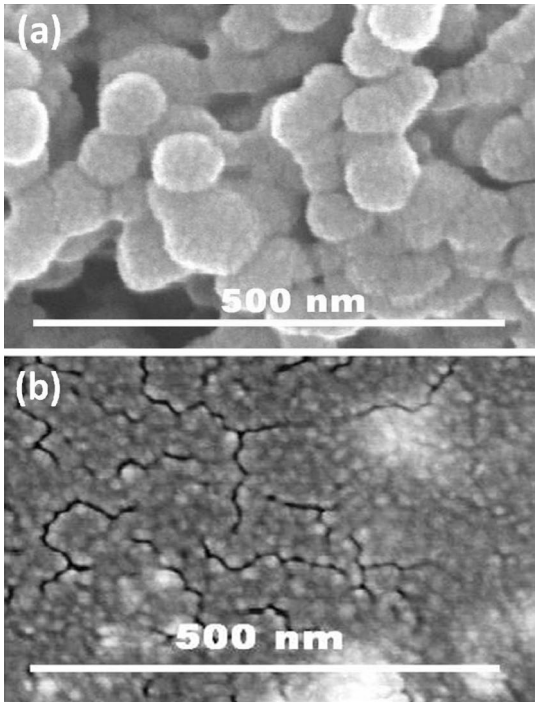

Fig. 4 FE-SEM images for **a** SNPs and **b** GNPs onto glass substrates

Procedure

Synthesis of silver and gold nanoparticles

Initially, 40 mL of 10 mM gold salt ($HAuCl_4$) and silver salt ($AgNO_3$) solutions were diluted in 360 mL deionized water. *Ficus racemosa* latex (0.5 mL) from natural source was dissolved in 5 mL of double-distilled water followed by filtering through 0.45 μ filter. Then filtrate was diluted to 10 mL from which 1 mL latex extract was added to initially prepare gold and silver solutions separately. Then Silver solution was kept in dark and gold solution was kept in sunlight for appropriate period (2 h). The color change of solutions from colorless to brown or black for silver and from light yellow to purple for gold indicated the synthesis of SNPs and GNPs, respectively (Fig. 1). These nanoparticles were subjected to purification by washing their aqueous colloidal solutions with 10 mL methanol and then washed nanoparticles were separated by centrifugation at 3,000 rpm for 1 h. This purification step was repeated for 3–4 times to attain maximum purity of synthesized nanoparticles and stored in methanol for further use.

Preparation for UV/Vis absorption measurements

Stock solutions with 10^{-2} M concentration of the following amino acids were prepared in deionized water: L-lysine monohydrochloride, L-arginine, L-glutamine, and glycin. Appropriate amounts of nanoparticles were weighed and transferred to distilled water separately. Then pH of this colloidal nanoparticles was adjusted to different pH conditions by the dropwise addition of 0.5 M HNO_3 or 0.5 M NH_3 under vigorous stirring. Generally, the pH conditions were set to alkaline (pH 8–9), neutral (pH 5.5–7), or acidic (pH 2–3). These pH-adjusted colloidal nanoparticles were diluted up to the mark using distilled water with desired pH to derive stock solutions of nanoparticles with concentrations 17.7 nM at different pH. Then for nanoparticles–amino acid complex preparation, different amounts in μL of the amino acids under investigation was added to the 3 mL aliquot of the nanoparticle solution at a given pH. These freshly mixed solutions were immediately placed into a 10-mm cuvette for the immediate reading of the UV/Vis spectrum. Then association constants were determined by the UV/Vis spectral changes using Benesi-Hildebrand method (Benesi and Hildebrand 1949; Tayade et al. 2014).

Association between nanoparticles and amino acids can be represented by Eq. (1).

$$\text{NPs} + \text{amino acid} \rightarrow \text{NPs} \cdot \text{amino acid}. \quad (1)$$

The corresponding association constant K can be defined by Eq. (2),

$$K = [\text{NPs} \cdot \text{amino acid}]/[\text{NPs}][\text{amino acid}] \quad (2)$$

and can be determined using the Benesi-Hildebrand equation which is shown in Eq. (3):

$$1/\Delta A = (1/(\varepsilon K))\,(1/[G]) + (1/\varepsilon), \quad (3)$$

where $[G]$ is the total of donor (amino acid),

ΔA is the absorbance difference between absorbance of initial nanoparticle solution and absorbance after formation of NPs·amino acid compex at maximum wavelength λ in nm,

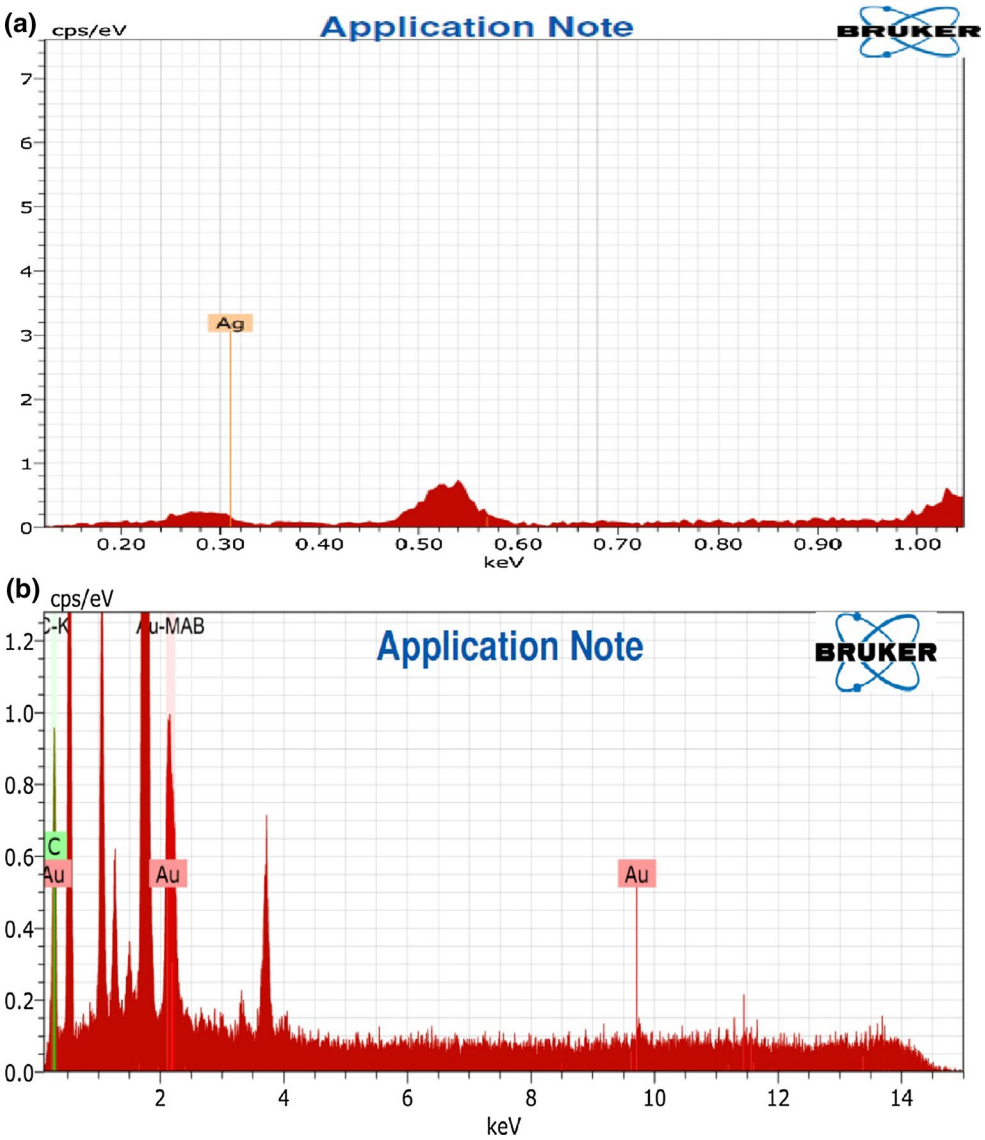

Fig. 5 EDS images for **a** SNPs and **b** GNPs

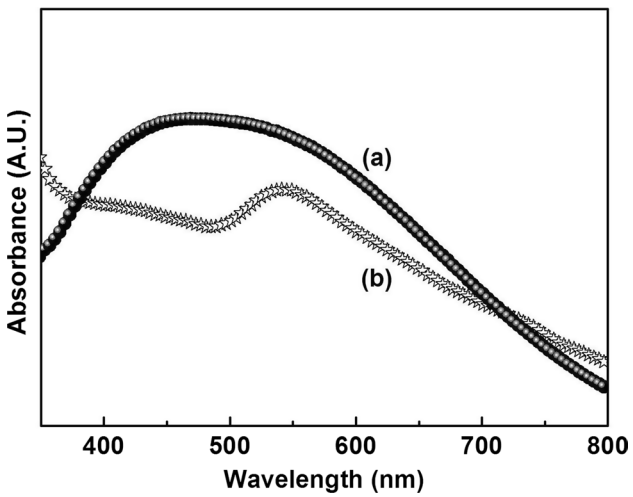

Fig. 6 UV/Vis Spectra for **a** SNPs and **b** GNPs after 2 h

K is the association constant for NPs·amino acid complex formation, and ε is the molar absorptivity of NPs·amino acid complex at maximum wavelength λ in nm. From Eq. (3), plot of $x = 1/[G]$ vs $y = 1/\Delta A$ gives a y-intercept $= 1/\varepsilon$ and slope $= (1/K_a\varepsilon)$ which gives the value of K_a.

Anticipated results

Reaction kinetics

Ficus racemosa is one of the important herbs due to its use in traditional system of medicine for the treatment of several disorders. The latex of this plant has many therapeutic uses such as in hemorrhoids, boils, alleviates the edema in adenitis, parotitis, orchitis, traumatic swelling, toothache, vaginal disorders, diarrhea particular in children, and also

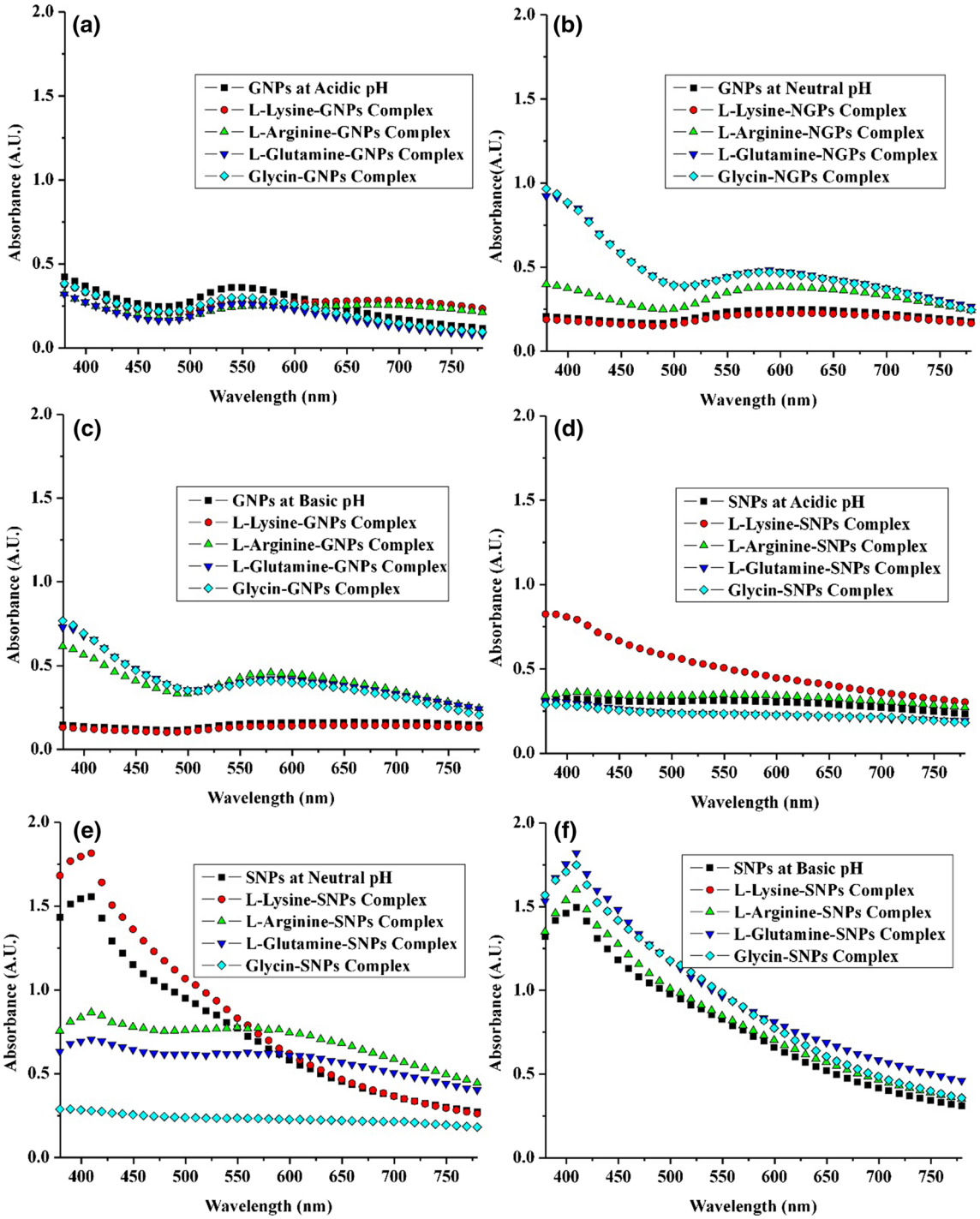

Fig. 7 UV/Vis spectra for different nanoparticle and amino acid complex formation at different pH conditions. Concentration of nanoparticles used for formation of complex = 17.7 nM and concentration of amino acids used for formation of complex = 0.164 mM. **a** GNPs and their complexes at acidic pH, **b** GNPs and their complexes at neutral pH, **c** GNPs and their complexes at basic pH, **d** SNPs and their complexes at acidic pH, **e** SNPs and their complexes at neutral pH and **f** SNPs and their complexes at basic pH

aphrodisiac (Shiksharthi and Mittal 2011). Latex is applied externally on chronic infected wounds to alleviate edema and pain and to promote the healing (Paarakh 2009). In spite of such extensive use of this plant in medicine, very little phytochemical work has been carried out. *Ficus racemosa* latex unusually contains thermo stable aspartic protease enzymes containing prominently β-structures (Devaraj et al. 2008). These enzymes are long single-chain

Table 1 Association constant (K) for nanoparticles and four amino acids at different pH conditions

	Association constant (K) (M^{-1})			
	L-Lysine	L-Arginine	L-Glutamine	Glycin
GNPs				
Acidic	4,410.7	5,764.2	5,498.7	1,691.6
Neutral	1,639.8	172.9	1,088.4	8,400.7
Basic	2,333.8	592.7	988.5	989.6
SNPs				
Acidic	6,322.0	1,695.7	1,467.6	2,202.2
Neutral	3,774.9	1,821.0	8,152.2	10,769.5
Basic	2,823.8	115.1	1,754.3	1,989.6

amino acids, with ~5 % sequence identity between all members of the family (Davies 1990). Aspartic protease can undergo oxidative cleavage by different processes such as radiolysis and metal-catalyzed oxidation which results in transfer of electrons to electron-deficient centers (Stadtman 1993). Possible mechanism for formation of these nanoparticles has been shown in Fig. 2. In this case, oxidative cleavage may be proceed through metal-catalyzed route for silver and radiolysis for gold as SNPs does not required any external energy and GNPs formed in presence of sunlight. Both these processes lead to release of free electrons which can be utilized for reduction of both silver and gold ions to their metallic states resulting in the formation of nanoparticles.

Structural studies

The typical powder XRD patterns of the prepared nanoparticles are shown in Fig. 3a for silver and Fig. 3b for gold. The data show diffraction peaks at $2\theta = 35.4°$, 37.5°, and 40.2° which can be indexed to (100), (002), and (101) planes for silver (PDF card no. 01-071-5025) which corresponds to hexagonal crystal structure, whereas Fig. 2b data show diffraction peaks at $2\theta = 38.3°$, 44.5°, and 64.8° which can be indexed to (111), (200), and (220) planes for gold (PDF card no. 00-002-1095) with cubic crystal structure. The average crystallite size of SNPs and GNPs was calculated using the well-known Debye–Scherrer's formula and found to be 95.49 and 44.15 nm, respectively. It confirmed the formation of SNPs and GNPs by green chemistry approach at room temperature.

Surface morphology and elemental analysis

Figure 4 shows FE-SEM images obtained for synthesized nanoparticles which are coated by dipping the glass substrate in the solution of respective solution. It is observed that the silver grains are in the size ranges of 50 to 120 nm which is an agglomeration of small crystallites observed as tiny dark and bright spots (Fig. 4a). On the other hand, well-covered GNPs are seen with average grain diameter ranging from 20 to 50 nm (Fig. 4b). EDX spectrum (Fig. 5a, b) shows peaks for silver and gold, which reveals the presence of SNPs and GNPs.

UV/Vis absorption studies

UV/Vis absorption spectra for SNPs and GNPs were recorded after 2 h and are shown in Fig. 6. SNPs shows broad absorption band over maximum visible range of 380 to 700 nm (Fig. 6a) with tiny absorption hump at 450 nm. This indicates that SNPs are the combination of nanoparticles of different sizes which was also observed in FE-SEM analysis, whereas GNPs resulted in strong absorption peak (λ_{max}) at 550 nm which indicates less size distribution. The GNPs gives absorption peak at 545 nm which lies in the visible region of the solar spectrum (Fig. 6b).

UV/Vis spectra of colloidal nanoparticles before and after addition of different amino acids at varying pH are shown in Fig. 7; all spectra exhibit a distinctive absorption peak for both nanoparticles with small shifts in wavelength depending on complex formation between nanoparticles and amino acids. These shifts in absorption peaks are size dependent of colloidal nanoparticles and occur due to change in the nanoparticle's dielectric environment, such as molecules binding to the surface of nanoparticle or nanoparticle aggregation. The dependence of the complex formation on pH values at acidic, neutral, and basic may be attributed to the change in ionic strength of the colloidal nanoparticle. Figure 7a shows decrease in absorption peak values for all GNPs-amino acids complexes which may be attributed to dilution effect, but for L-lysine and L-arginine new broad absorption peaks are observed at whole visible region and higher values of association constant (K) as compared to other pH conditions (Table 1) suggest good binding between GNPs with all four amino acids under study at acidic condition. Figure 7b, c demonstrates the binding of four amino acids with GNPs at neutral and basic pH, and results show the increase in absorption values for L-arginine, L-glutamine, and glycin due to complex formation with GNPs at neutral and basic pH. However, at same pH conditions L-lysine does not show significant change in absorption peaks over visible range. From Fig. 7d–f and Table 1, it can be seen that SNPs shows good binding at acidic and neutral conditions as compared to basic conditions with all four amino acids. This is due to decrease in stability of SNPs itself at basic conditions.

Figure 8 shows schematic diagram for association of these four binding acids with nanoparticles at different pH conditions. Amino acids arrange their charge with respect to pH conditions which affects the binding of these amino acids

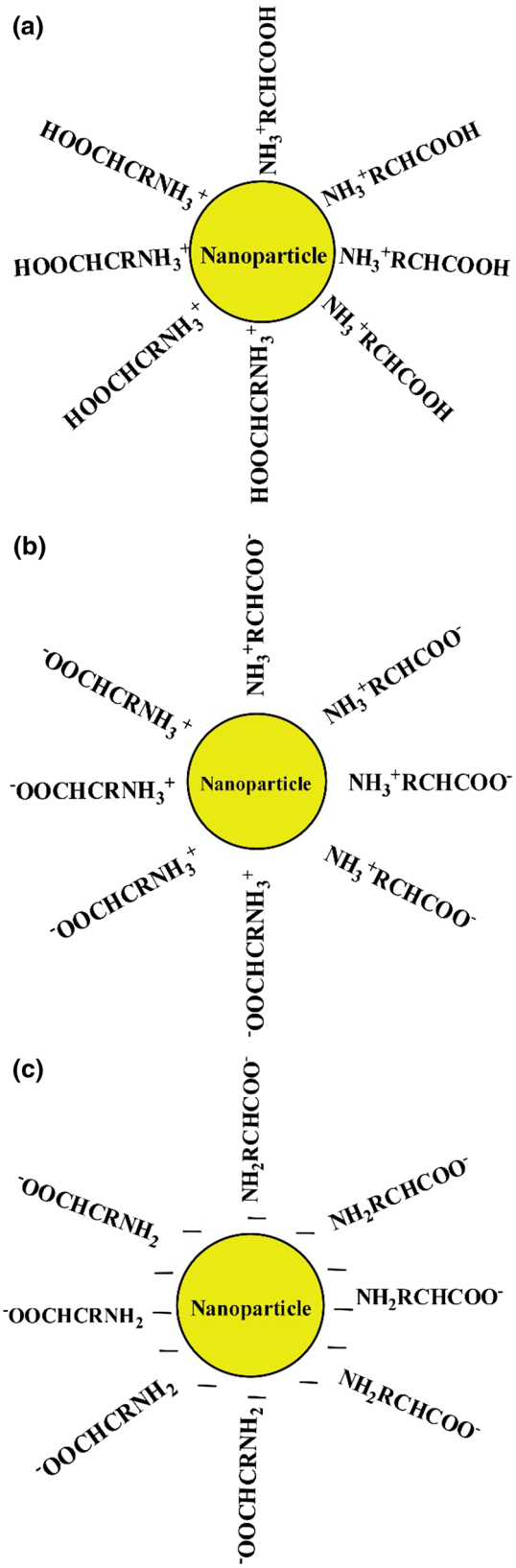

Fig. 8 Schematic diagram of association of nanoparticles with amino acids at **a** acidic, **b** neutral, and **c** basic conditions

with nanoparticles. At low (acidic) pH, COO^- group and NH_2 groups are protonated to COOH and NH_3^+. The association of amino acid and nanoparticles is faster at lower pH, which is due to the effect of protonating the carboxyl and amino groups. This is the good condition for both nanoparticles to bind these amino acids through amine groups. At neutral pH, amino acids generally present as zwitterions which contain both positive and negative charges and due to this amino acids assemble themselves in definite pattern and this makes poor condition as compared to acidic condition for binding with nanoparticles. However, at higher (basic) pH, amino acids contain COO^- and NH_2 to which nanoparticles cannot bind because of the negative charge of COO^- group.

Conclusion

The green chemistry approach through natural source *Ficus racemosa* latex as a reducing agent to reduce silver and gold cations to SNPs and GNPs, respectively, is successfully demonstrated at room temperature. The use of natural source without the use of toxic precursors as biological synthesis was shown to be rapid and produces particles of fairly uniform size and shape which can be applied for large-scale applications. The binding studies of SNPs and GNPs with four amino acids, namely L-lysine, L-arginine, L-glutamine, and glycin have shown that this type of binding is pH dependent. This complex formation study between GNPs and SNPs at different pH will make it possible to design different nanostructures as biosensors.

Acknowledgments This work was supported by Grants from UGC (University Grant Commission), New Delhi, Government of India. We are thankful to Central Instrumentation Laboratory, University Institute of Chemical Technology, North Maharashtra University, Jalgaon, for providing FE-SEM and XRD instrumentation facilities.

Conflict of interest The authors have no conflicts of interest to disclose.

References

Alric C, Taleb J, Duc GL, Mandon C, Billotey C, Meur-Herland AL, Brochard T, Vocanson F, Janier M, Perriat P, Roux S, Tillement O (2008) Gadolinium chelate coated gold nanoparticles as contrast agents for both x-ray computed tomography and magnetic resonance imaging. J Am Chem Soc 130:5908–5915

Armendariz V, Herrera I, Peralta-Videa JR, Jose-Yacaman M, Troiani H, Santiago P, Gardea-Torresdey JL (2004) Size controlled gold nanoparticle formation by *Avena sativa* biomass: use of plants in nanobiotechnology. J Nanopart Res 6:377–382

Basavegowda N, Sobczak-Kupiec A, Malina D, Yathirajan HS, Keerthi VR, Chandrashekar N, Dinkar S, Liny P (2013) Plant mediated synthesis of gold nanoparticles using fruit extracts of

ananas comosus (L.) (pineapple) and evaluation of biological activities. Adv Mat Lett 4:332–337
Benesi HA, Hildebrand JH (1949) A spectrophotometric investigation of the interaction of iodine with aromatic hydrocarbons. J Am Chem Soc 71:2703–2707
Bryaskova R, Pencheva D, Kyulavska M, Bozukova D, Debuigne A, Detrembleur C (2010) Antibacterial activity of poly(vinyl alcohol)-b-poly(acrylonitrile) based micelles loaded with silver nanoparticles. J Colloid Interface Sci 344:424–428
Cai W, Ting G, Hao H, Jiangtao S (2008) Applications of gold nanoparticles in cancer nanotechnology. J Nanotechnol Sci Appl 1:17–32
Christensen L, Vivekanandhan S, Misra M, Mohanty AK (2011) Biosynthesis of silver nanoparticles using *murraya koenigii* (*curry leaf*): an investigation on the effect of broth concentration in reduction mechanism and particle size. Adv Mat Lett 2:429–434
Das RK, Brar SK (2013) Plant mediated green synthesis: modified approaches. Nanoscale 5:10155–10162
Davies DR (1990) The structure and function of the aspartic proteinases. Annu Rev Biophys Biophys Chem 19:189–215
De S, Kundu R, Biswas A (2012) Synthesis of gold nanoparticles in niosomes. J Colloid Interface Sci 386:9–15
Devaraj KB, Gowda LR, Prakash V (2008) An unusual thermostable aspartic protease from the latex of *Ficus racemosa* (L.). Phytochemistry 69:647–655
Dipankar C, Murugan S (2012) The green synthesis, characterization and evaluation of the biological activities of silver nanoparticles synthesized from *Iresine herbstii* leaf aqueous extracts. Colloids Surf B 98:112–119
Dong C, Zhang X, Cai H (2014) Green synthesis of monodisperse silver nanoparticles using hydroxyl propyl methyl cellulose. J Alloys Compd 583:267–271
Du L, Xian L, Feng JX (2011) Rapid extra-/intracellular biosynthesis of gold nanoparticles by the fungus *Penicillium* sp. J Nanopart Res 13:921–930
Gardea-Torresdey JL, Parsons JG, Dokken K, Peralta-Videa J, Troiani HE, Santiago P, Jose-Yacaman M (2002) Formation and growth of au nanoparticles inside live *alfalfa* plants. Nano Lett 2:397–401
Gardea-Torresdey JL, Gomez E, Peralta-Videa JR, Parsons JG, Troiani H, Jose-Yacaman M (2003) *Alfalfa sprouts*: a natural source for the synthesis of silver nanoparticles. Langmuir 19:1357–1361
Huang J, Li Q, Sun D, Lu Y, Su Y, Yang X, Wang H, Wang Y, Shao W, He N, Hong J, Chen C (2007) Biosynthesis of silver and gold nanoparticles by novel sundried *Cinnamomum camphora* leaf. Nanotechnology 18:105104–105115
Justin Packia Jacob S, Finub JS, Narayanan A (2012) Synthesis of silver nanoparticles using *Piper longum* leaf extracts and its cytotoxic activity against Hep-2 cell line. Colloids Surf B 91:212–214
Kasthuri J, Kathiravan K, Rajendiran N (2009) Phyllanthin-assisted biosynthesis of silver and gold nanoparticles: a novel biological approach. J Nanopart Res 11:1075–1085
Khalil MMH, Ismail EH, El-Baghdady KZ, Mohamed D (2013) Green synthesis of silver nanoparticles using *olive* leaf extract and its antibacterial activity. Arab J Chem. doi:10.1016/j.arabjc.2013.04.007 (article in press)
Li S, Shen Y, Xie A, Yu X, Qiu L, Zhang L, Zhang Q (2007) Green synthesis of silver nanoparticles using *Capsicum annuum* L. extract. Green Chem 9:852–858
Mihailescu GH, Olenic L, Pruneanu S, Bratu I, Kacso I (2007) The effect of pH on amino acids binding to gold nanoparticles. J Optoelectron Adv M 9:756–759
Mittal AK, Bhaumik J, Kumar S, Banerjee UC (2014) Biosynthesis of silver nanoparticles: elucidation of prospective mechanism and therapeutic potential. J Colloid Interface Sci 415:39–47
Narayanan KB, Sakthivel N (2008) Coriander leaf mediated biosynthesis of gold nanoparticles. Mater Lett 62:4588–4590
Nazeruddin GM, Prasad NR, Waghmare SR, Garadkar KM, Mulla IS (2014) Extracellular biosynthesis of silver nanoparticle using *Azadirachta indica* leaf extract and its anti-microbial activity. J Alloys Compd 583:272–277
Paarakh PM (2009) *Ficus racemosa* linn.—an overview. Nat Prod Radiance 8:84–90
Rajasekharreddy P, Rani PU, Sreedhar B (2010) Qualitative assessment of silver and gold nanoparticle synthesis in various plants: a photobiological approach. J Nanopart Res 12:1711–1721
Rao YS, Kotakadi VS, Prasad TNVKV, Reddy AV, Gopal DVRS (2013) Green synthesis and spectral characterization of silver nanoparticles from *Lakshmi tulasi* (*Ocimum sanctum*) leaf extract. Spectrochim Acta Part A 103:156–159
Reddy PR, Rani PU, Sreedhar B (2010) Qualitative assessment of silver and gold nanoparticle synthesis in various plants: a photobiological approach. Nanopart J Res 12:1711–1721
Sathyavathi R, Krishna MB, Rao SV, Saritha R, Rao DN (2010) Biosynthesis of silver nanoparticles using *coriandrum sativum* leaf extract and their application in nonlinear optics. Adv Sci Lett 3:1–6
Shiksharthi AR, Mittal S (2011) *Ficus Racemosa*: phytochemistry, Traditional Uses and Pharmacological Properties: A Review. Int J Recent Adv Pharm Res 4:6–15
Shukla VK, Singh RP, Pandey AC (2010) *Black pepper* assisted biomimetic synthesis of silver nanoparticles. J Alloys Compd 507:L13–L16
Singh AK, Talat M, Singh DP, Srivastava ON (2010) Biosynthesis of gold and silver nanoparticles by natural precursor clove and their functionalization with amine group. J Nanopart Res 12:1667–1675
Song JY, Kim BS (2009) Rapid biological synthesis of silver nanoparticles using plant leaf extracts. Bioprocess Biosyst Eng 32:79–84
Song JY, Jang HK, Kim BS (2009) Biological synthesis of gold nanoparticles using *Magnolia Kobus* and *Diopyros kaki* leaf extracts Process. Biochem 44:1133–1138
Stadtman ER (1993) Oxidation of free amino acids and amino acid residues in proteins by radiolysis and by metal-catalyzed reactions. Annu Rev Biochem 62:797–821
Tayade KC, Kuwar AS, Fegade UA, Sharma H, Singh N, Patil UD, Attarde SB (2014) Design and synthesis of a pyridine based chemosensor: highly selective fluorescent probe for pb(II). J Fluoresc 24:19–26
Thakkar KN, Mhatre SS, Parikh RY (2010) Biological synthesis of metallic nanoparticles. Nanomed Nanotechnol 6:257–262
Vivek R, Thangam R, Muthuchelian K, Gunasekaran P, Kaveri K, Kannan S (2012) Green biosynthesis of silver nanoparticles from *Annona squamosa* leaf extract and its in vitro cytotoxic effect on MCF-7 cells. Process Biochem 47:2405–2410
Zare D, Akbarzadeh A, Bararpour N (2010) Synthesis and functionalization of gold nanoparticles by using of poly functional amino acids. Int J Nanosci Nanotechnol 6:223–230